

# On Energy Compaction of 2D Saab Image Transforms

Na Li\*, Yongfei Zhang<sup>†</sup>, Yun Zhang\*, C.-C. Jay Kuo<sup>‡</sup>

\* Shenzhen Institutes of Advanced Technology, Chinese Academy of Sciences, Shenzhen, China

<sup>†</sup> School of Computer Science and Engineering, Beihang University, Beijing, China

<sup>‡</sup> University of Southern California, Los Angeles, California, USA

**Abstract**—The block Discrete Cosine Transform (DCT) is commonly used in image and video compression due to its good energy compaction property. The Saab transform was recently proposed as an effective signal transform for image understanding. In this work, we study the energy compaction property of the Saab transform in the context of intra-coding of the High Efficiency Video Coding (HEVC) standard. We compare the energy compaction property of the Saab transform, the DCT, and the Karhunen-Loeve transform (KLT) by applying them to different sizes of intra-predicted residual blocks in HEVC. The basis functions of the Saab transform are visualized. Extensive experimental results are given to demonstrate the energy compaction capability of the Saab transform.

## I. INTRODUCTION

Two-dimensional (2D) image transforms map 2D signals defined on a regular grid from the spatial domain to the spectral domain. Since they can compact the energy distribution in the spatial-domain to a fewer number of frequency-domain coefficients, 2D image transforms are widely used in image or video coding standards. Traditionally, 2D image transforms adopt separable transform kernels. That is, the 2D transform kernel is formed by the tensor product of horizontal and vertical one-dimensional (1D) transform kernels. The transforms are first conducted along one dimension (say, the horizontal dimension) and then followed in the second dimension (say, the vertical dimension).

It is well known that the Karhunen-Loeve transform (KLT) is the optimal transform in the sense that it provides the best energy compaction property. To derive the 1D KLT, we first compute the covariance matrix of image pixels in one horizontal or vertical segment of  $N$  pixels (say,  $N = 4, 8, 16, 32$ , etc.). Next, we find the eigenvectors of the covariance matrix, which are the KLT basis functions. The KLT is also known as the principal component analysis (PCA). The KLT is a data-dependent (or data-driven) transform, which has higher computational complexity than data-independent transforms. The discrete cosine transform (DCT) [6] is a data-independent transform, which can be easily implemented by hardware for acceleration. Besides, the DCT provides a good approximation to data-dependent KLT for image data. The 2D separable DCT is widely used in today's image and video coding standards.

We compare the energy compaction property of the Saab transforms with the DCT and the KLT in the context of intra-coding of the High Efficiency Video Coding (HEVC) standard

[8] in this work. Our research objective is to enhance the DCT performance by exploring three new directions.

### 1) Data-independent versus data-dependent transforms

Generally speaking, data-dependent transforms such as the PCA have better energy compaction property than data-independent transforms such as the DCT. However, data-dependent transforms received little attention in the past due to their higher computational complexity. However, it is a recent trend in modern video coding standards to trade higher computational complexity for a higher coding gain. Thus, it is worthwhile to revisit data-dependent transforms.

### 2) Separable versus nonseparable transforms [7], [9]

Most existing higher dimensional transforms are derived as the tensor product of several 1D transforms. However, this may not be the optimal choice. It is actually easy to derive high dimensional transforms directly. Let us use the 2D case as an example. For an image block of size  $N \times N$ , we can concatenate  $N$  pixels in  $N$  rows into one long vector of length  $N^2$  and compute the covariance matrix for such random vectors accordingly. The eigenvectors of the covariance matrix define a set of 2D nonseparable transform kernels. We would like to check whether a 2D nonseparable transform is better than its corresponding 1D separable transform in energy compaction.

### 3) One-stage versus multi-stage transforms

By factorizing  $N$  into the product of two integers, *i.e.*,  $N = N_1 \times N_2$ , we can conduct two-stage PCA. The first stage PCA is applied to a segment of  $N_1$  pixels. There are  $N_2$  segments in total. We obtain  $N_1$  transform coefficients for each segment. In the second stage, we conduct the PCA on a data array of dimension  $N_1 \times N_2$ , where  $N_1$  and  $N_2$  indicate the numbers of frequency and spatial components. The output is still of dimension  $N = N_1 \times N_2$ . One example of multi-stage PCA is the Saab transform proposed by Kuo *et al.* in [1]. The main feature of the Saab transform is to add a sufficiently large constant to all output elements from the previous transform stage so that all input elements to the next stage PCA are non-negative. This is needed to avoid the sign confusion problem. There is little comparison study between one-stage and multi-stage PCA in the

literature [2]. Here, we would like to see whether the Saab transform (*i.e.*, multi-stage PCA) has a better energy compaction property than one-stage PCA.

We conduct extensive experimental results to demonstrate that the Saab transform outperforms both the DCT and the PCA in terms of energy compaction efficiency. This makes it an attractive candidate in future image/video coding standards.

The rest of this paper is organized as follows. Background is reviewed in Sec. II. We examine the energy compaction property of the DCT, the PCA and the Saab transform on different sizes of intra-predicted residual blocks in HEVC in Sec. III. The basis functions of the Saab transform are visualized in Sec. IV. Concluding remarks are given in Sec. V.

## II. BACKGROUND REVIEW

Transform energy compaction means the capability of a transform to redistribute signal energy into a smaller number of transform coefficients. Among state-of-the-art separable transforms, the DCT is the most widely used in the compression field, including the JPEG image coding standard and MPEG-1, MPEG-2, H.264/AVC and HEVC video coding standards. For example, in the latest HEVC coding standard, the DCT is applied to both intra and inter block residuals of size  $N \times N$ , where  $N = 4, 8, 16$  and  $32$ . It is followed by quantization and entropy coding. The kernel functions of the 2D DCT are in form of

$$f(m, n) = \frac{2}{N} \sum_{p=0}^{N-1} \sum_{q=0}^{N-1} \Lambda(p) \Lambda(q) \cos\left(\frac{(2p+1)\pi m}{2N}\right) \cos\left(\frac{(2q+1)\pi n}{2N}\right), \quad (1)$$

where  $m, n = 0, \dots, N-1$  and  $\Lambda(\xi) = \sqrt{2}^{-1}$  if  $\xi = 0$  and  $1$ , otherwise.

To consider dependency of row and column elements of a picture [7], one can arrange pixel samples in an image block of size  $N \times N$  in lexicographic order; namely,

$$\mathbf{x} = [x_{00}, x_{01}, \dots, x_{0,N-1}, x_{10}, x_{11}, \dots, x_{1,N-1}, \dots, x_{N-1,0}, \dots, x_{N-1,N-1}]^T. \quad (2)$$

Similarly, we can express a transform kernel as

$$\mathbf{a} = [a_{00}, a_{01}, \dots, a_{0,N-1}, a_{10}, a_{11}, \dots, a_{1,N-1}, \dots, a_{N-1,0}, \dots, a_{N-1,N-1}]^T. \quad (3)$$

One can conduct the PCA on random vectors as defined by Eq. (2) and choose the principal components as the kernels in Eq. (3).

Pixels in images have a decaying correlation property. The correlation between local pixels is stronger and the correlation becomes weaker as their distance becomes larger. To exploit this property, Kuo *et al.* [1] conducted a subspace affine transform in a local window to get a local spectral vector. The input space is first decomposed into the DC (direct current) subspace and the AC (alternate current) subspace in the Saab transform. The AC subspace is formed by elements

$$\mathbf{x}_{AC} = \mathbf{x} - (\mathbf{a}_0^T \mathbf{x} + b_0) \mathbf{1}, \quad (4)$$

where  $\mathbf{1} = \mathbf{c}/\|\mathbf{c}\|$ , and  $\mathbf{c} = (1, 1, \dots, 1, 1)$  is the constant unit vector, in each stage of the Saab transform. The block Saab transform is given by [1]

$$y_k = \sum_{n=0}^{N^2-1} a_{k,n} x_n + b_k = \mathbf{a}_k^T \mathbf{x} + b_k \quad k = 0, 1, \dots, N^2 - 1, \quad (5)$$

where  $\mathbf{a}_0$  is the DC filter and  $\mathbf{a}_k$ ,  $k = 1, \dots, N^2 - 1$  are the AC filters. The PCA is adopted to compute the AC filters in the AC subspace. The bias term  $b_k$ ,  $k = 0, 1, \dots, N^2 - 1$  is selected to be a sufficiently large positive number to ensure that  $\mathbf{x}_{AC}$  is non-negative when it serves as the input to the Saab transform in the next stage.

We would like to emphasize the main differences between the KLT and the Saab transform below.

- The KLT does not decompose signals into DC and AC components. It removes the ensemble mean and then compute the eigen-vectors of the covariance matrix of mean-removed signals. The Saab transform has one default DC filter. Then, we conduct the PCA on DC-removed signals.
- The input to the KLT can be positive and negative values while the input to any stage in the Saab transform should always be non-negative.

The Saab transform proposed by Kuo *et al.* [1] is a data-driven (PCA-based), multi-stage, and nonseparable transform. It meets all three criteria stated in Sec. I. The Saab transform is motivated by the analysis of nonlinear activation of convolutional neural networks (CNNs) in [3], [4] as well as the subspace approximation interpretation of convolutional filters in [5]. We will focus on the energy compaction property of the 2D Saab image transform in this preliminary study and show that it offers better energy compaction capability than the DCT and the KLT. Thus, it is an attractive image transform candidate for image and video compression.

To make our study as close to the real world coding environment as possible, we study the energy compaction capability of several transforms applied to block residuals obtained by intra prediction in the HEVC test model version 16.9 under the all intra configuration in the next section.

We consider non-overlapping blocks with the following settings.

- block size  $4 \times 4$   
For the one-stage transform, we map 16 pixels in one block to one direct current (DC) coefficient and 15 alternating current (AC) coefficients. For the two-stage transform, we first map one subblock of size  $2 \times 2$  to one DC and 3 AC coefficients. Afterwards, we map a spatial-spectral cuboid, which has a spatial dimension of  $2 \times 2$  and a spectral dimension of 4, to a spectral vector of dimension 16. Again, it has one DC and 15 AC coefficients.
- block size  $8 \times 8$   
For the one-stage transform, we map 64 pixels in one block to one DC coefficient and 63 AC coefficients. For the two-stage transform, we consider two cases. For the

first case, we first map one subblock of size  $2 \times 2$  to one DC and 3 AC coefficients. After that, we map a spatial-spectral cuboid, which has a spatial dimension of  $4 \times 4$  and a spectral dimension of 4, to a spectral vector of dimension 64. For the second case, we first map one subblock of size  $4 \times 4$  to one DC and 15 AC coefficients. Afterwards, we map a spatial-spectral cuboid, which has a spatial dimension of  $2 \times 2$  and a spectral dimension of 16, to a spectral vector of dimension 64. In both of the cases, it has one DC and 63 AC coefficients.

- block size  $16 \times 16$

For the one-stage transform, we map 256 pixels in one block to one DC coefficient and 255 AC coefficients. For the two-stage transform, we first map one subblock of size  $4 \times 4$  to one DC and 15 AC coefficients. Afterwards, we map a spatial-spectral cuboid, which has a spatial dimension of  $4 \times 4$  and a spectral dimension of 16, to a spectral vector of dimension 256, which contains one DC and 255 AC coefficients.

### III. ENERGY COMPACTION COMPARISON OF IMAGE TRANSFORMS

We compare the energy compaction properties of the DCT, the KLT and the one-stage and two-stage Saab transforms in this section. First, we describe the energy compaction measure and elaborate on how to collect block residuals from the HEVC encoder and obtain the Saab transform kernels accordingly in Sec. III-A. Then, we compare the energy compaction property of different transforms applied to intra-predicted block residuals of various sizes and resolutions in HEVC in Sec. III-B.

#### A. Energy Compaction Measure and Sample Number Selection

The Saab transform kernels are computed from the covariance matrix, which will converge statistically as the number of samples increases. We need to determine the number of samples required by the covariance matrix computation. A covariance matrix is said to converge if the Frobenius-norm difference of two covariance matrices sampled by  $M$  and  $M'$  samples ( $M \approx M'$ ) becomes sufficiently small, *e.g.*, less than  $\epsilon = 1.5 \times 10^{-4}$ .

An example of the relationship between the covariance matrix difference computation and the number of samples is shown in Fig. 1, where the y-axis is the Frobenius-norm difference of two covariance matrices expressed in the natural log scale and the x-axis indicates the sample numbers. This plot is obtained using the  $8 \times 8$  luminance (Y) residual blocks for sequence “BasketballDrive” of frame resolution  $832 \times 480$ , encoded by HM version 16.9 under all intra configuration with four quantization parameter (QP) values (*i.e.*, 22, 27, 32 and 37). To compute the Saab transform kernels (or the KLT eigenvectors), we see from the figure that it is sufficient to use around 60K blocks for the covariance matrix to converge as Frobenius-norm difference of two covariance matrices is to be less than  $\epsilon = 1.5 \times 10^{-4}$ . We adopt the same process

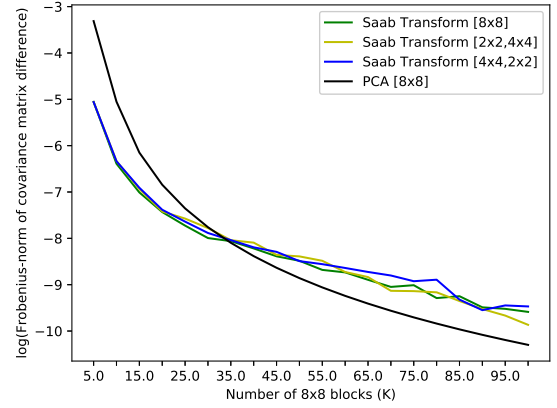


Fig. 1. Determination of the sample number required for Saab transform kernel computation for the luminance (Y) block of size  $8 \times 8$ .

in deriving Saab transform kernels and KLT eigenvectors for block sizes with different resolutions.

By energy compaction, we refer to the capability of a transform to redistribute the signal energy into a small number of transform coefficients. For a block of dimension  $N \times N$ , we obtain  $N^2$  transform coefficients. For the DCT and the Saab transform, the first one is the DC coefficient while the remaining ones are the AC coefficients. Although the KLT does not decompose signals into the DC and AC subspaces, there is an equivalent concept; namely, its ensemble mean component. The KLT subtracts the ensemble mean from all signals and then compute the principal vectors on the mean-removed signal subspace. It is not practical to compute the ensemble mean in image and video coding so that we use the spatial mean to estimate the ensemble mean under the ergodic assumption. By following the above condition, we show the averaged DC energy ( $k = 0$ ), the AC energy ( $1 \leq k \leq 15$ ) and the total energy ( $0 \leq k \leq 15$ ) for 100 luminance (Y) block residuals of size  $4 \times 4$  in Table I, where the component  $k = 0$  in the KLT is the energy of the ensemble mean vector.

TABLE I  
AVERAGED DC AND AC ENERGY VALUES FOR LUMINANCE (Y) RESIDUAL BLOCKS OF SIZE  $4 \times 4$  UNDER DIFFERENT TRANSFORMS.

Energy	Index (k)	DCT	KLT	Saab Transform	
				[4× 4]	[2× 2, 2× 2]
DC	0	122.35	150.29	122.35	49.53
AC	1~15	155.56	127.02	155.19	228.20
Total	0~15	277.90	277.31	277.54	277.73

Although there are small variations in the total energy values, the difference becomes smaller as the sample size becomes larger. Theoretically, the total energy before and after all orthonormal transforms should be the same. Since the DCT and the one-stage Saab transform compute the DC components of blocks in the same manner, they have the same averaged DC values. The KLT has the highest energy for  $k = 0$ . However, their differences become smaller as the number of residual

block samples increases as shown in Fig. 2. Asymptotically, they all converge to zero since we expect the residual blocks should be averaged out in the long run.

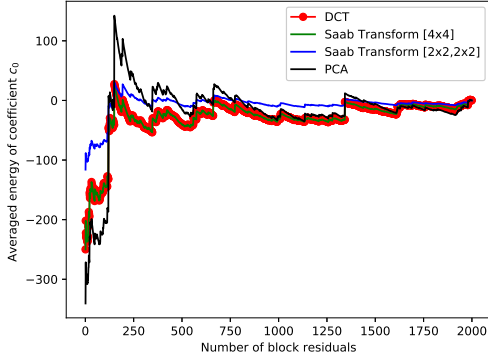


Fig. 2. Comparison of averaged energy of the coefficient indexed  $k = 0$  of DCT, KLT, the one-stage and the two-stage Saab transforms as a function of the number of residual blocks.

Interestingly, the two-stage Saab transform has the lowest DC energy among the four in Table I. At the second-stage Saab transform, its DC computation involves the sum of a cuboid of four spatial dimensions and four spectral dimensions. Only the lowest spectral dimension of the four spatial locations contribute significant energy values. Thus, after averaging, its DC value drops. Since the DC component has no discriminant power in image classification, the multi-stage Saab transform is preferred for pattern recognition and computer vision applications. In the context of image and video coding, DC and AC components are encoded separately. We expect the DC coding cost is the lowest for the two-stage Saab transform.

When the number of block samples increase, the ensemble mean of the KLT will converge to the DC value. As a result, the KLT, the DCT and the one-stage Saab transform will have the same value for  $k = 0$ . The AC energy compaction is the only determining factor for the total energy compaction. In contrast, the DC component of the two-stage Saab transform is significantly smaller. The larger range of AC energy is good for recognition. However, it is still not clear whether this helps or hurts the overall RD gain. It demands further study. If we show both DC and AC in one plot, we cannot see the excellent AC energy compaction of the two-stage Saab transform clearly since it is masked by its low DC value. For this reason, we focus on the energy compaction property of a transform of its AC coefficients only (*i.e.*,  $K = 1, \dots, N^2 - 1$  for  $N^2$  coefficients) below. Mathematically, we have

$$E_K^{N \times N} = \frac{\sum_{k=1}^K c_k^2}{\sum_{k=1}^{N^2-1} c_k^2} \times 100\%, \quad (6)$$

where  $c_k$  is the coefficient of the  $k$ th AC component of the transform.

## B. Energy Compaction Performance Comparison

We compare the AC energy compaction performance of the DCT, the KLT, one-stage and two-stage Saab transforms. We will discuss the luminance (Y) block residuals first and, then, the chrominance red (Cr) block residuals.

**Luminance Blocks of Size  $4 \times 4$ .** We first examine residuals for blocks of size  $4 \times 4$ . They are obtained via intra prediction coded with  $QP = 22$  and predicted as the planar mode. The cumulative AC energy is plotted as a function of first  $K$  AC coefficients in Fig. 3 (a). The curves indicate the mean values of four different transforms. We see that the DCT, the KLT and the one-stage Saab transform have similar AC energy compaction property while the two-stage Saab transform outperforms all of them by a significant margin. The advantage of two-stage Saab transform on the cumulative AC energy is demonstrated via sequences “FourPeople”, “BasketballDrive” and “PeopleOnStreet” of resolutions  $1280 \times 720$ ,  $1920 \times 1080$  and  $2560 \times 1600$  in Figs. 3 (b)–(d).

**Luminance Blocks of Size  $8 \times 8$ .** We examine luminance (Y) block residuals of size  $8 \times 8$  for four video sequences with the intra predicted planar mode; namely, “BasketballDrill”, “FourPeople”, “BasketballDrive” and “PeopleOnStreet”. The AC cumulative energy plots in Figs. 4(a)–(d). We have two observations. First, the two-stage Saab transforms have better AC energy compaction property than the DCT, the KLT and the one-stage Saab transform. Two cases of the two-stage Saab transform are compared: 1)  $2 \times 2$  spatial blocks followed by  $4 \times 4$  spatial blocks and 2)  $4 \times 4$  spatial blocks followed by  $2 \times 2$  spatial blocks. Case (2) is slightly better than case (1).

**Luminance Blocks of Size  $16 \times 16$ .** We plot the AC energy compaction of luminance (Y) block residuals of size  $16 \times 16$  with the intra predicted planar mode for four video sequences of different resolutions in Figs. 5(a)–(d). The two-stage Saab transform with  $4 \times 4$  spatial blocks followed by  $4 \times 4$  spatial blocks has the best AC energy compaction property among all benchmarking cases.

**Chrominance Blocks of Sizes  $8 \times 8$  and  $16 \times 16$ .** The AC energy compaction properties for residuals of intra predicted chrominance red (Cr) blocks for sequence “BasketballDrive” are compared in Figs. 6(a)(b). The differences between different transforms are smaller for chrominance red (Cr) block residuals.

## IV. VISUALIZATION OF TRANSFORM BASIS FUNCTIONS

We can gain additional insights into image transforms by visualizing their basis functions (or transform kernels). To obtain the one-stage or the two-stage Saab transform basis functions, we set one and only one AC spectral component in the last stage to unity while setting other AC spectral components to zero. Afterwards, we perform the inverse one-stage or two-stage Saab transform from the spectral domain back to the spatial domain. Finally, we normalize the gray level of each pixel to the range between 0 and 255 using a linear scaling operation followed by a shifting operation.

**Luminance Blocks of Size  $4 \times 4$ .** We compare the basis functions of the DCT, the one-stage Saab transform and the

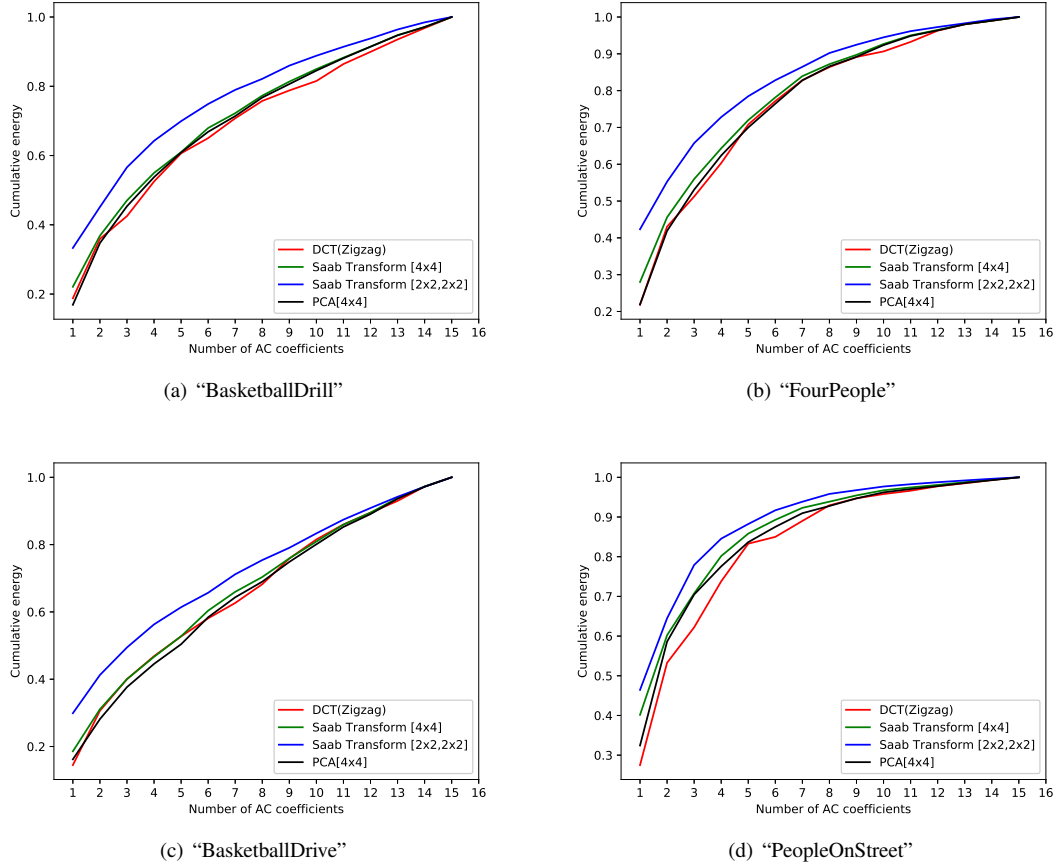


Fig. 3. The cumulative AC energy plot for luminance (Y) block residuals of size  $4 \times 4$  for four video sequences: (a)“BasketballDrive” of resolution  $832 \times 480$ , (b)“FourPeople” of resolution  $1280 \times 720$ , (c)“BasketballDrill” of resolution  $1920 \times 1080$ , and (d)“PeopleOnStreet” of resolution  $2560 \times 1600$ .

two-stage Saab transform with the planar mode in Fig. 7. Since the DCT is a separable transform, we show the transform basis functions in form of a 2D array in Fig. 7(a), where the upper left corner is the DC component while the other 15 are AC components. We see that separability of transform kernels imposes severe constraints on the kernel form. Since the Saab transform is a nonseparable one, their transform kernels for DC is followed by AC kernels, where AC kernels are ordered from the largest to the smallest energy percentages, in two rows (*i.e.*, from left to right and then from top to bottom). The basis function of the one-stage Saab transform are shown in Fig. 7(b). The first AC basis is in bowl form, the second and the third AC basis functions are tilted planes of 135 and 45 degrees, respectively, the fourth one is in saddle form and the fifth one is in well form. These patterns are more likely to happen. The remaining basis functions are less frequently seen. Finally, we show the basis function of the two-stage Saab transform Fig. 7(c). The first AC of the two-stage Saab transform is in bowl form but rotated by 45 degree. The most interesting observation is the last three AC components. The two-stage Saab transform can include them in the basis function set. This is the major difference between the one-stage and the two-stage Saab transforms.

**Luminance Blocks of Size  $8 \times 8$ .** We show the basis functions of the one-stage Saab transform for luminance residual blocks of size  $8 \times 8$  with the intra horizontal mode and the intra planar mode in Figs. 8 (a) and (b), respectively. When a block is predicted to be in the horizontal mode, it tends to have textures along the horizontal direction. Thus, the first 8 AC basis functions in Fig. 8(a) all have horizontal patterns so as to express the signal better. This is not possible for DCT basis functions. When a block is predicted to be in the planar mode, the basis functions can be in bowl shape, tilted planes, saddle shape, *etc.*.

**Luminance Blocks of Size  $16 \times 16$ .** We show the basis functions of the two-stage Saab transform for luminance (Y) block residuals of size  $16 \times 16$  with the intra horizontal mode and the intra planar mode in Figs. 9 (a) and (b), respectively. We have observations similar to  $8 \times 8$  blocks with the intra horizontal mode and the intra planar mode as studied above.

## V. CONCLUSION AND FUTURE WORK

The energy compaction property of the multi-stage non-separable data-driven Saab transform was studied on different block residual sizes for intra prediction in HM version 16.9 in this work. It was demonstrated by extensive experimental

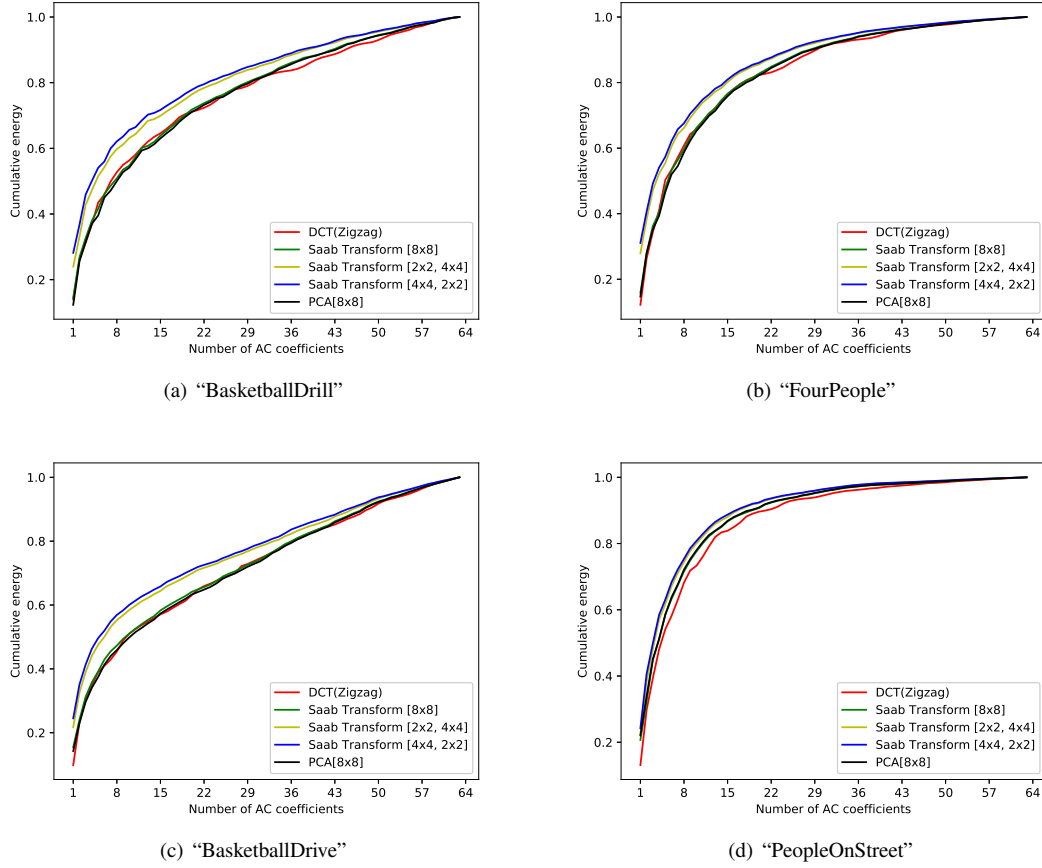


Fig. 4. The cumulative AC energy plot for luminance (Y) block residuals of size  $8 \times 8$  for video sequences: (a)“BasketballDrill” of resolution  $832 \times 480$ , (b)“FourPeople” of resolution  $1280 \times 720$ , (c)“BasketballDrive” of resolution  $1920 \times 1080$ , and (d)“PeopleOnStreet” of resolution  $2560 \times 1600$ .

results that the Saab transform has better energy compaction capability than the widely used DCT and PCA. Thus, we can draw the conclusion that the Saab transform offers a highly competitive solution to the residual transform for future image/video coding standards. Furthermore, the basis functions of the Saab and DCT were visualized and compared. This helps explain the advantages of the Saab transform over the DCT and the PCA.

It is desired to extend our study to block residuals of inter prediction. Besides, we plan to incorporate the quantization and the entropy coding modules and provide a complete picture of the rate-distortion gain of the Saab transform over the DCT in the HEVC video coding standard in the near future.

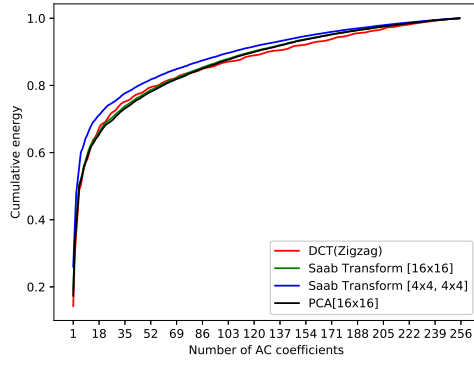
#### ACKNOWLEDGMENT

This work was supported in part by Shenzhen International Collaborative Research Project under Grant GJHZ20170314155404913 and Guangdong International Science and Technology Collaborative Research Project under Grant 2018A050506063. This work was also supported in part by the National Natural Science Foundation of China (No. 61772054) and the NSFC Key Project (No. 61632001).

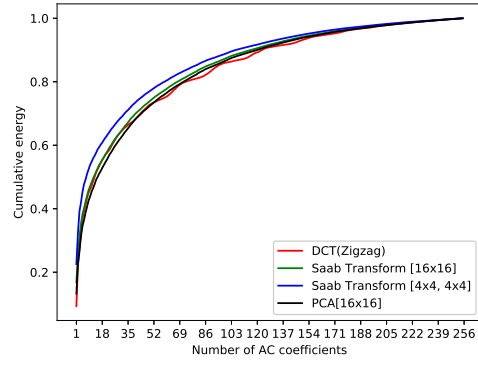
#### REFERENCES

- [1] C.-C. J. Kuo, M. Zhang, S. Li, J. Duan, and Y. Chen, “Interpretable convolutional neural networks via feedforward design,” in *Journal of Visual Communication and Image Representation*, pp.346-359, 2019.
- [2] Y. Su, R. Lin, and C.-C. J. Kuo, “Tree-structured multi-stage principal component analysis (TMPCA): Theory and applications,” *Expert Systems with Applications* 118 (2019): 355-364.
- [3] C.-C. J. Kuo, “Understanding convolutional neural networks with a mathematical model,” in *Journal of Visual Communication and Image Representation*, vol.41, pp.406-413, 2016.
- [4] C.-C. J. Kuo, “The CNN as a guided multilayer RECOS transform [lecture notes],” in *IEEE Signal Processing Magazine*, vol.34, no.3, pp.81-89, 2017.
- [5] C.-C. J. Kuo, Y. Chen, “On data-driven Saak transform,” in *Journal of Visual Communication and Image Representation*, vol.50, pp.237-246, 2018.
- [6] N. Ahmed, T. Natarajan and K.R. RAO, “Discrete Cosine Transform,” *IEEE Transaction on computers*, January 1974.
- [7] T. Raj Natarajan and N. Ahmed, “Performance Evaluation for Transform Coding Using a Nonseparable Covariance Model,” in *IEEE Transactions on Communications*, vol. 26, no. 2, pp. 310-312, February 1978.
- [8] G. J. Sullivan, J. Ohm, W.-J. Han, T. Wiegand, “Overview of the high efficiency video coding (HEVC) standard,” in *IEEE Transactions on Circuits and Systems for Video Technology*, 22, pp.1649C1668, December 2012.
- [9] J. A.D. Aston, D. Pigoli and S. Tavakoli, “Tests for separability in nonparametric covariance operators of random surfaces,” in *The Annals of Statistics*, vol.45, no.4, pp.1431-1461, 2017.

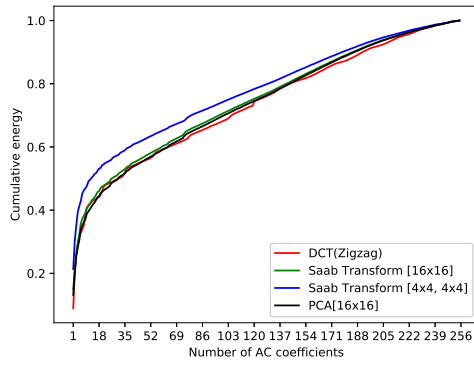




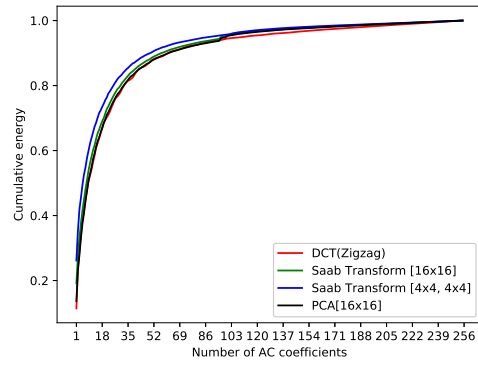
(a) “BasketballDrill”



(b) “FourPeople”

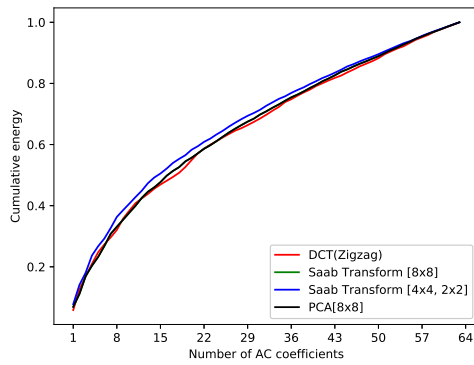


(c) “BasketballDrive”

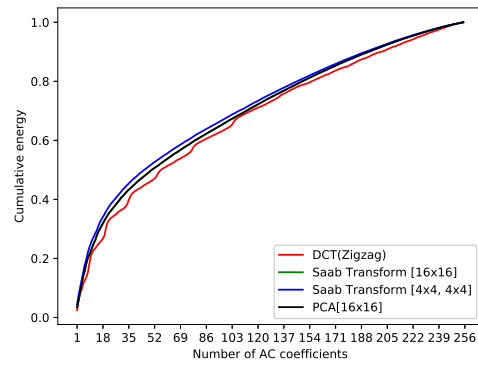


(d) “PeopleOnStreet”

Fig. 5. The cumulative AC energy plot for luminance (Y) block residuals of size  $16 \times 16$  for four video sequences: (a) “BasketballDrill” of resolution  $832 \times 480$ , (b) “FourPeople” of resolution  $1280 \times 720$ , (c) “BasketballDrive” of resolution  $1920 \times 1080$ , and (d) “PeopleOnStreet” of resolution  $2560 \times 1600$ .



(a)  $8 \times 8$  chrominance red (Cr) block



(b)  $16 \times 16$  chrominance red (Cr) block

Fig. 6. The cumulative AC energy plot for block Cr residuals under the intra prediction mode for “BasketballDrive” of resolution  $1920 \times 1080$  with block size: (a)  $8 \times 8$  and (b)  $16 \times 16$ .

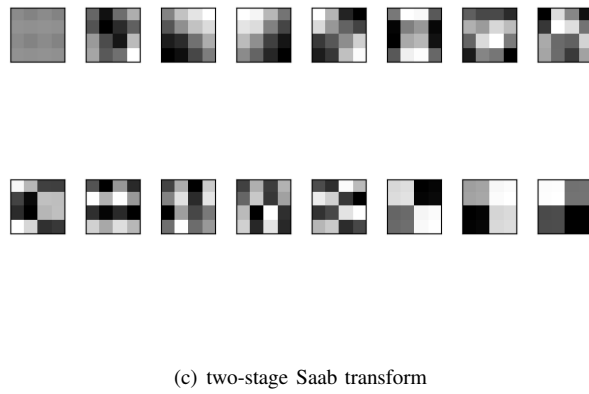
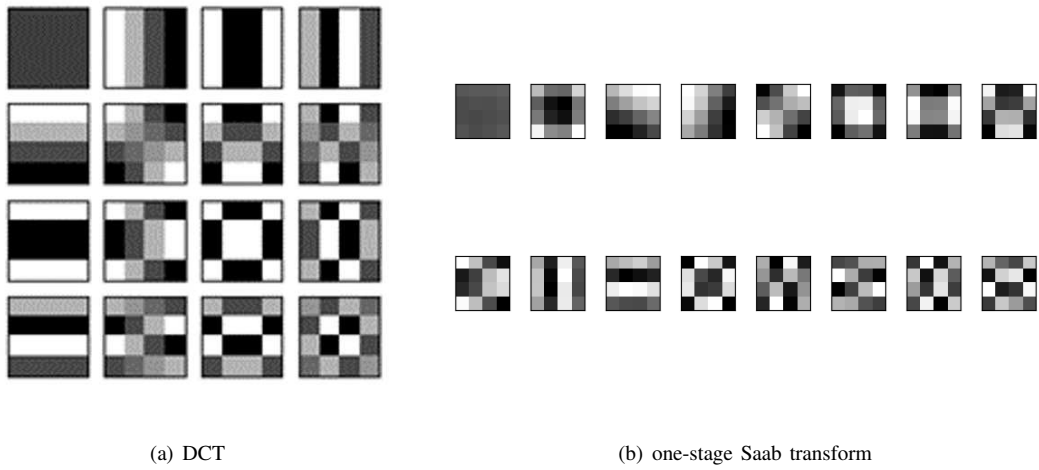
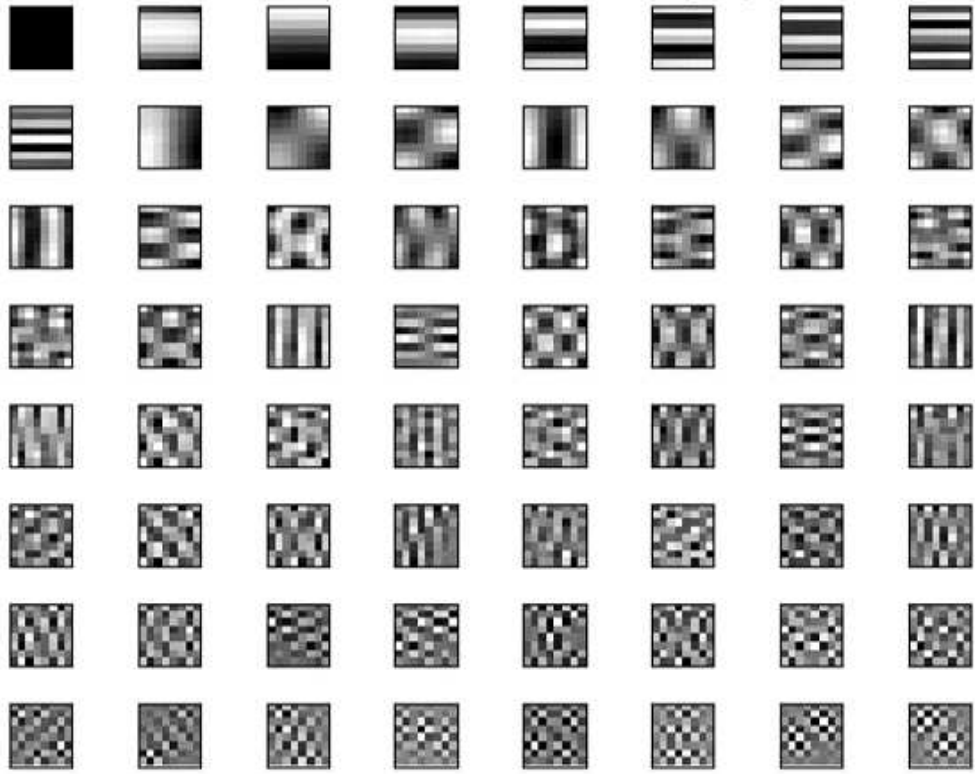
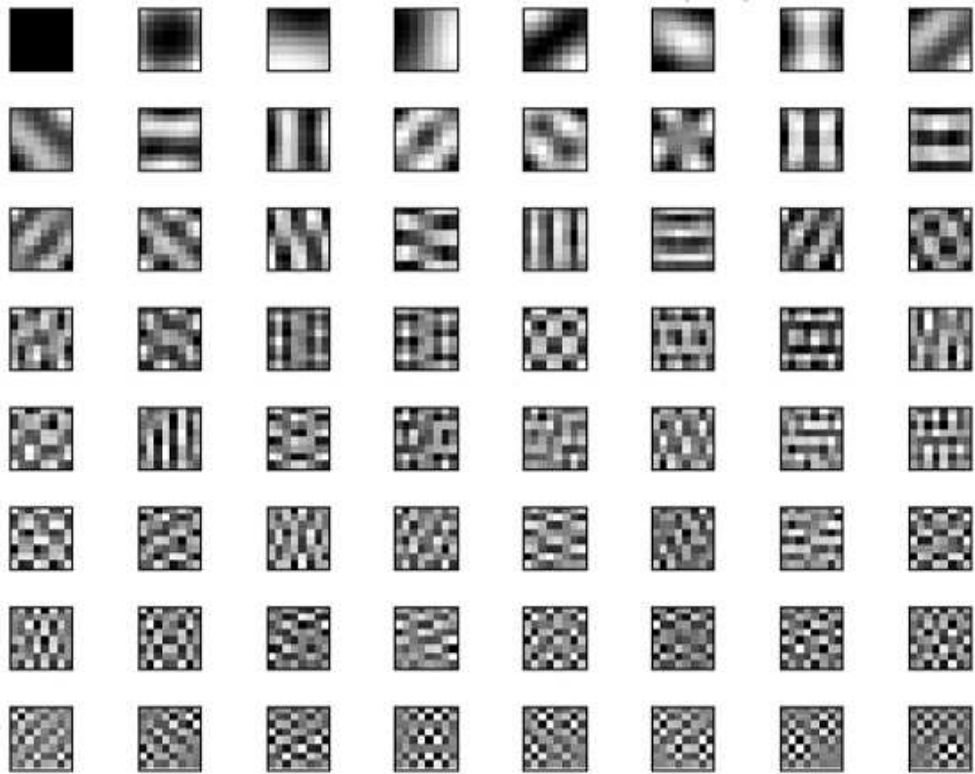


Fig. 7. Visualization of transform basis functions for  $4 \times 4$  blocks: (a) the DCT, (b) the one-stage Saab transform, and (c) the two-stage Saab transform.



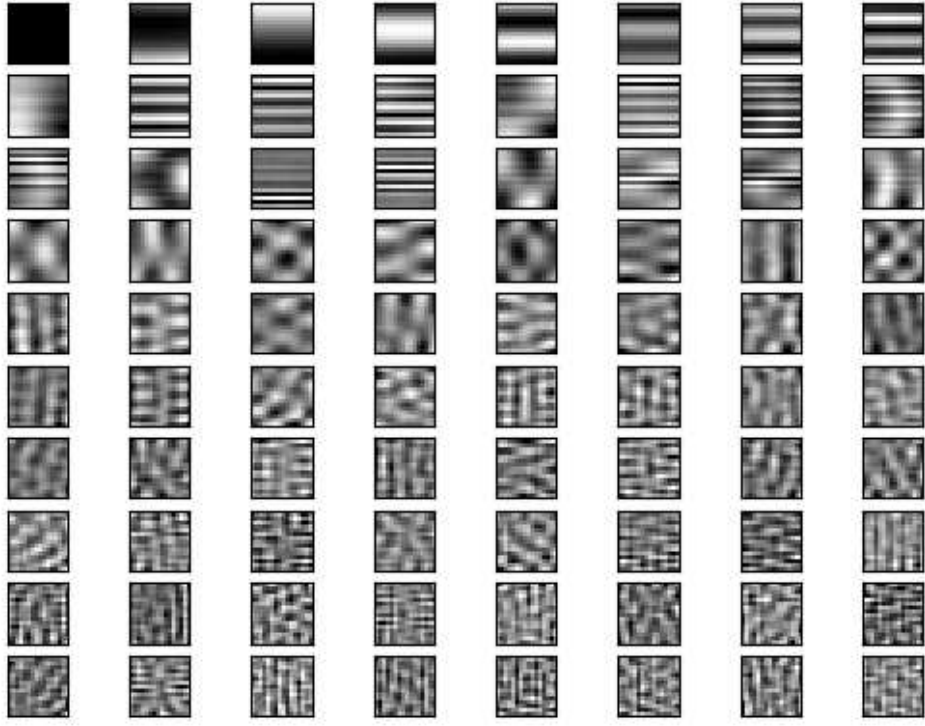


(a) intra horizontal

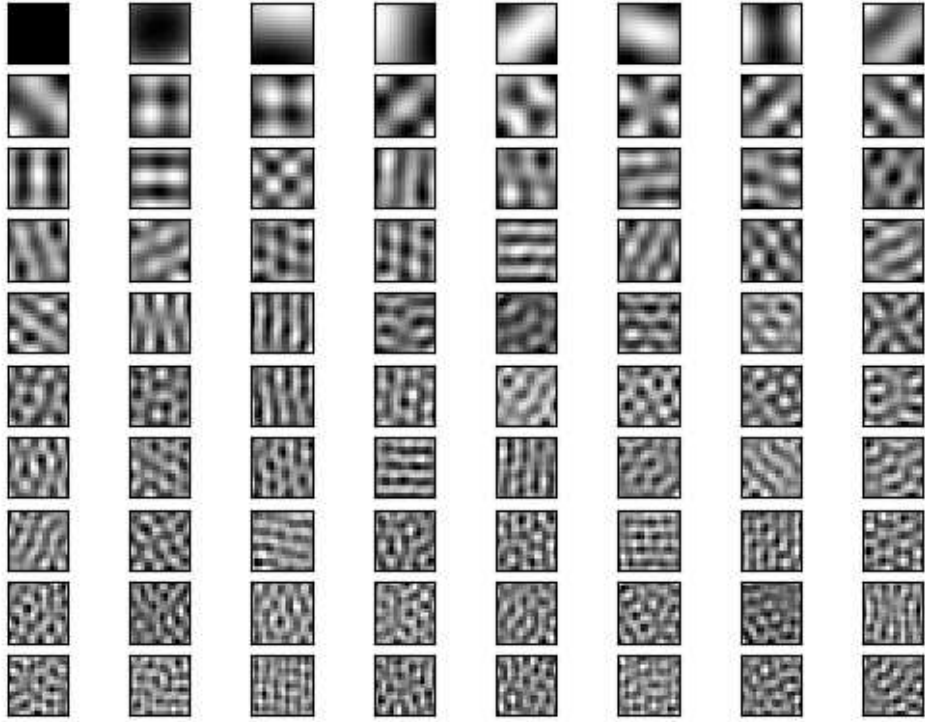


(b) intra planar

Fig. 8. Visualization of basis functions of the one-stage Saab transform for  $8 \times 8$  residual blocks with (a) the intra horizontal mode and (b) the intra planar mode.



(a) intra horizontal



(b) intra planar

Fig. 9. Visualization of the top 80 basis functions of the two-stage Saab transform for  $16 \times 16$  luminance residual blocks with (a) the intra horizontal and (b) the intra planar modes.